Plasmonics (2013) 8:85–92
DOI 10.1007/s11468-012-9425-6

Fluorescent (Au@SiO_2)SiC Nanohybrids: Influence of Gold Nanoparticle Diameter and SiC Nanoparticle Surface Density

Ning Sui · Virginie Monnier · Yuriy Zakharko · Yann Chevolot · Sergei Alekseev · Jean-Marie Bluet · Vladimir Lysenko · Eliane Souteyrand

Received: 14 May 2012 / Accepted: 6 August 2012 / Published online: 18 August 2012

Abstract Gold@silica core–shell nanoparticles were prepared with various gold core diameters (ranging from 20 to 150 nm) and silica thicknesses (ranging from 10 to 30 nm). When the gold diameter is increased, the size dispersion became larger, leading to a broader plasmon band. Then, silicon carbide (SiC) nanoparticles were covalently immobilized onto silica to obtain hybrid (Au@SiO_2) SiC nanoparticles. The absorption properties of these hybrid nanoparticles showed that an excess of SiC nanoparticles in the dispersion can be identified by a strong absorption in the UV region. Compared to SiC reference samples, a blue shift of the fluorescence emission, from 582 to 523 nm, was observed, which was previously attributed to the strong surface modification of SiC when immobilized onto silica. Finally, the influence of several elaboration parameters (gold diameter, silica thickness, SiC concentration) on fluorescence enhancement was investigated. It showed that the highest enhancements were obtained with 10 nm silica thickness, low concentration of SiC nanoparticles, and surprisingly, with a 20-nm gold core diameter. This last result could be attributed to the broad plasmon band of big gold colloids. In this case, SiC emission strongly overlapped gold absorption, leading to possible quenching of SiC fluorescence by energy transfer.

Keywords Fluorescence · Plasmon · Hybrid · Enhancement · Silicon carbide

N. Sui · V. Monnier (✉) · Y. Chevolot · E. Souteyrand
Institut des Nanotechnologies de Lyon—INL, UMR CNRS 5270,
Site Ecole Centrale de Lyon, Université de Lyon,
36 Avenue Guy de Collongue,
69134 Ecully, Cedex, France
e-mail: virginie.monnier@ec-lyon.fr

Y. Zakharko · J.-M. Bluet · V. Lysenko
Institut des Nanotechnologies de Lyon—INL, UMR CNRS 5270,
Site INSA Lyon, Université de Lyon,
7 Avenue Jean Capelle,
69621 Villeurbanne Cedex, France

S. Alekseev
Faculty of Chemistry, Kiev National Taras Schevchenko University,
64 Vladimirskaya St.,
01601 Kiev, Ukraine

Introduction

Plasmon-controlled fluorescence has become a powerful tool to monitor the optical properties of fluorescent emitters, located in the vicinity of a metal surface or a metal colloid [1–3]. However, the oscillating electrons of the metal plasmon can provoke either fluorescence enhancement or quenching depending on the nature of the metal and fluorescent emitter [4, 5], the separation distance between them [4, 6, 7], and the nature of spacer material [6, 8, 9], underlying the need to carefully control these parameters.

Several kinds of fluorescent emitters were investigated: organic dyes [5], quantum dots [6], or rare-earth oxides [7]. More recently, coupling between metal plasmon and fluorescent nanoparticles from group IV (carbon, silicon, and silicon carbide) has been reported [10–14]. These nanoparticles have several interesting features for fluorescent enhancement. Their emission wavelength depends strongly on

excitation wavelength, and they exhibit broad absorption and emission bands. As a consequence, an excellent overlap between their absorption/emission spectrum and plasmon band of the metal can be obtained [10]. This is a required condition to obtain effective metal-enhanced fluorescence. In particular, when excited at a 488-nm wavelength, SiC nanoparticles exhibit a broad fluorescence spectrum centered at 582 nm. This emission spectrum can overlap the 20- to 150-nm-diameter gold nanoparticle plasmon band.

Previously, we have elaborated and characterized new hybrid nanoparticles consisting of a gold core covered with a silica shell. On this silica shell, silicon carbide (SiC) nanoparticles were covalently immobilized [12]. The influence of silica thickness was studied. It was demonstrated that for a 25-nm-thick silica shell and a gold core of 20 nm in diameter, a maximum enhancement was obtained when the excitation wavelength was as close as possible to the gold plasmon band.

Herein, (Au@SiO_2)SiC hybrid nanoparticles with different gold core diameters, different silica thicknesses, and different SiC surface densities were synthesized. The influence of gold core diameter and of SiC nanoparticle surface density on fluorescent enhancement was investigated. Structural characterization was achieved; then, absorption and fluorescence properties were studied.

Experimental

Chemicals

Gold colloids of 20 and 150 nm in diameter were purchased from British BioCell International. Gold colloids of 60 nm in diameter were synthesized according to an already reported procedure [15]. Gold tetrachlorohydrate ($HAuCl_4$) and trisodium citrate were provided by Sigma-Aldrich. Tetra ethyl orthosilicate (TEOS), 3-aminopropyltrimethoxysilane (APTMS), sodium silicate solution ($Na_2(SiO_2)_{3–5}$, 27 wt% SiO_2), ethanol, tetrahydrofuran (THF), and ammonia solution (25–28 %) were purchased from Sigma-Aldrich. *N*, *N*′-diisopropylcarbodiimide (DIC) and *N*-hydroxysuccinimide (NHS) were obtained from Fluka. Milli-Q water (18.2 MΩ) was used in all the preparations.

Synthesis of Au@SiO_2 Nanoparticles

The synthesis of Au@SiO_2 nanoparticles was achieved following reported procedures [16, 17] with some modifications.

Synthesis of Au-20 nm@SiO_2 Nanoparticles A freshly prepared aqueous solution of APTMS (14.5 μL, 1 mM) was added to a commercial 20-nm gold colloid dispersion (5 mL, 7×10^{11} particles/mL) under vigorous magnetic stirring. After 15 min, a 0.54-wt% sodium silicate solution (200 μL) was added to this dispersion which was stirred for an additional 24 h. At this step, gold nanoparticles with a thin silica shell (~2 nm) could be collected by centrifugation (960×*g* for 1 h). Next, these nanoparticles were transferred to a 1:5 water/ethanol mixture (6 mL); 125 μL of ammonia solution and TEOS were added. The volume of TEOS was set to 0.75 and 2.5 μL to obtain 10 and 25 nm silica thicknesses, respectively. This dispersion was allowed to react overnight under mild magnetic stirring. The product was separated by centrifugation at 10,600×*g* for 10 min and finally dispersed in 5 mL of ethanol.

Synthesis of Au-60 nm@SiO_2 Nanoparticles Sixty-nanometer gold colloids were first prepared by reduction of $HAuCl_4$ salt by trisodium citrate [15]. A 0.01-wt% $HAuCl_4$ solution (50 mL) was heated to reflux. Three-hundred microliters of a trisodium citrate solution (1 wt%) was added. The solution turned to blue then to red–purple in 2 min. The reaction was continued for 30 min. The silica coating on Au-60 nm was achieved through a modified Stöber process [17]. Five milliliters of ethanol, 125 μL of ammonia solution, and TEOS were added to 1 mL of gold colloid dispersion in water (2.3×10^{10} nanoparticles/mL). The volume of TEOS was set to 2.5 μL to obtain a 30-nm silica thickness. This dispersion was allowed to react overnight under mild magnetic stirring. The product was separated by centrifugation at 10,600×*g* for 10 min and finally redispersed in 5 mL of ethanol.

Synthesis of Au-150 nm@SiO_2 Nanoparticles The preparation of Au-150 nm@SiO_2 nanoparticles was similar to the synthesis of Au-60 nm@SiO_2. One microliter of TEOS was added to a mixture of ethanol (5 mL) and gold colloid dispersion (1 mL, 1.7×10^9 nanoparticles/mL) to obtain a 15-nm-thick silica shell.

Preparation and Size Selection of SiC Nanoparticles

SiC nanoparticles were prepared by a previously reported method based on electrochemical etching [18]. The obtained SiC nanopowder was dispersed in water and then centrifuged at 4,900×*g* for 3 min in order to sediment large crystallites at the bottom of the centrifugation tube and to collect the useful top part from the supernatant containing nanoparticles with a diameter ranging between 1 and 3 nm. These nanoparticles are highly stable in water. Finally, the concentration of SiC dispersion was set to 1 gL^{-1}.

Surface Functionalization of Au@SiO_2 Nanoparticles with Amino Groups

Au@SiO_2 nanoparticles were functionalized with APTMS using a reported method [19]. Various amounts of a 1-mM

APTMS solution in ethanol were added to Au@SiO_2 nanoparticle dispersion depending on their diameter. Experimental conditions are summarized in Table 1.

Preparation of (Au@SiO_2)SiC Nanoparticles

To achieve the covalent immobilization of SiC nanoparticles onto Au@SiO_2 nanoparticles, 200 μL of Au@SiO_2-NH_2 nanoparticles (containing 1.4×10^{11} nanoparticles) was mixed with various amounts of SiC nanoparticle dispersion (1 gL^{-1} in water). Then, the mixture was dried under vacuum, and dry THF containing NHS and DIC (at a molar ratio of NHS/DIC= 1:2.5) was added. The mixture was refluxed at 60 °C for 4 h. (Au@SiO_2)SiC nanoparticles were purified by centrifugation, and the precipitate was finally dispersed in a 1:1 water/ethanol mixture for characterization.

Characterization

SEM images were obtained with a Tescan microscope working at 10 kV. For SEM, samples were prepared by the deposition of 2 μL of the Au@SiO_2 nanoparticle dispersion on a silicon wafer substrate. UV–visible absorption spectra were obtained on a SAFAS UV mc2 double-beam spectrophotometer using a micro-cuve of 1 mm length containing 5 μL of dispersion to analyze.

Argon-ion laser emitting at λ=488 nm was used to obtain room temperature fluorescence spectra. The dispersions were poured into UV transparent quartz recipients. To evaluate the metal effect on SiC nanoparticle fluorescence, a reference consisting of SiC nanoparticles in a 1:1 water/ethanol mixture was used. For enhancement factor calculation, the concentration of this reference was set to the same concentration added for the elaboration of (Au@SiO_2)SiC nanoparticles. The enhancement factor was calculated by the ratio between the fluorescence intensities of (Au@SiO_2)SiC and SiC nanoparticles, at two different emission wavelengths (λ_{em}=523 nm and λ_{em}=582 nm). These two wavelengths correspond to the maximum emission of (Au@SiO_2)SiC nanoparticles and SiC nanoparticles, respectively [12].

Results and Discussion

Synthesis of Au@SiO_2 Nanoparticles

Several methods were used for the synthesis of Au@SiO_2 nanoparticles depending on the core diameter and the targeted silica thickness. The growth of a silica shell on small gold colloids (diameter lower or equal to 20 nm) generally requires the use of a two-step process involving (1) the formation of a thin silica layer (~2 nm) around gold colloids and (2) the growth of a thicker silica layer by classical Stöber process [16, 17]. The first step is necessary to obtain homogeneously silica-coated gold colloids. Indeed, due to their small diameter, gold colloids are submitted to strong attractive Van der Waals interactions, which can induce coalescence of gold colloids during the silica shell growth. These interactions are shielded by the 2-nm silica layer. Thus, it allows the growth of silica shell by Stöber process without coalescence during the second step. Concerning bigger gold colloids (diameter higher than 20 nm), the silica shell growth can be performed directly by Stöber method. Indeed, in this case, Van der Waals interactions are weaker; thus, the silica shell growth can be performed directly without any preliminary surface modification of gold colloids.

SEM images (Fig. 1) showed that a homogeneous silica coating was obtained for all gold diameters. Smaller gold colloids (diameter, 20 nm) were all spherical (Fig. 1a and b), while bigger colloids (diameters 60 and 150 nm) had more heterogeneous shapes (Fig. 1c and d). Several long colloids were observed when the gold diameter was 60 nm (Fig. 1c), while long and triangular shapes were observed when the gold diameter was 150 nm (Fig. 1d). Nanoparticle formation occurs in several steps: (1) nucleation for a very short time, (2) growth of the nuclei, and (3) Ostwald ripening (dissolution of smaller particles and redeposition of the dissolved species on larger particles) [20]. The dissolution of smaller clusters is strongly influenced by the surface curvature of already formed nanoparticles: the higher the curvature, the higher the dissolution rate. Thus, for bigger nanoparticles, dissolution is negligible compared to aggregation, allowing

Table 1 Experimental conditions for Au@SiO_2 nanoparticle amino-functionalization

Au@SiO_2 nanoparticle samples (Au-core diameter@SiO_2-silica thickness)	Concentration of Au@SiO_2 nanoparticle dispersion (nanoparticles/mL)	Volume of Au@SiO_2 nanoparticle dispersion (mL)	Volume of 1 mM APTMS solution (μL)
Au-20 nm@SiO_2-10 nm	7×10^{11}	1	20
Au-20 nm@SiO_2-25 nm	7×10^{11}	1	50
Au-60 nm@SiO_2-30 nm	2.3×10^{10}	1	5
Au-150 nm@SiO_2-15 nm	1.7×10^{9}	1	2

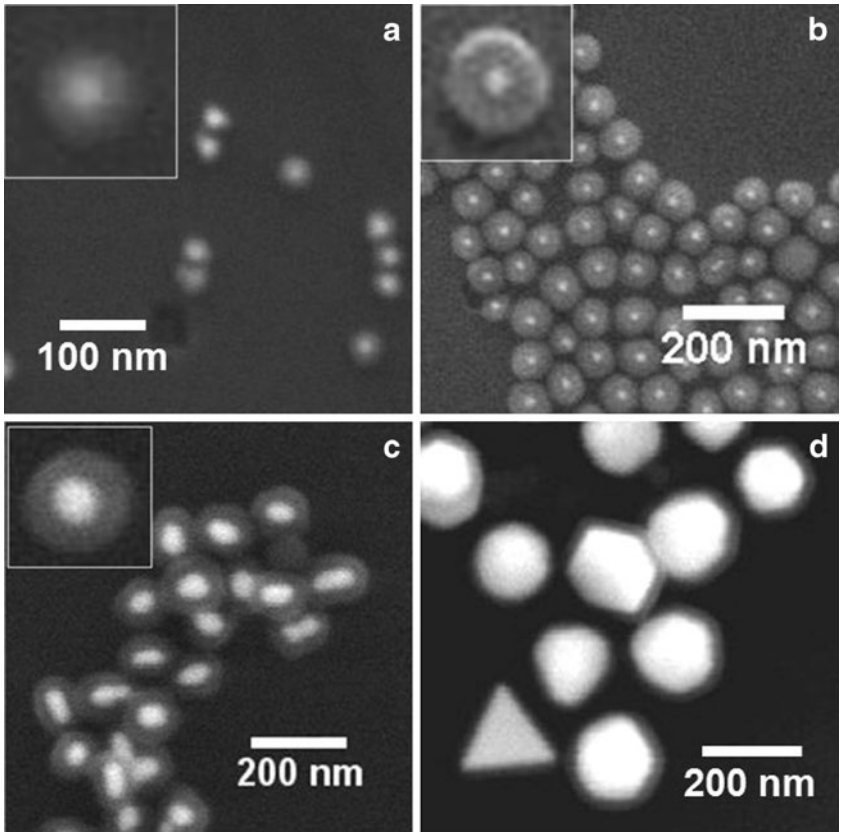

Fig. 1 SEM images of $Au@SiO_2$ nanoparticles with various gold core diameters and silica shell thicknesses: **a** Au-20 nm@SiO_2-10 nm, **b** Au-20 nm@SiO_2-25 nm, **c** Au-60 nm@SiO_2-30 nm, and **d** Au-150 nm@SiO_2-15 nm. The *insets* show high-magnification images on a single nanoparticle

the development of low-energy crystal faces, rather than keeping the spherical shape of the nuclei. However, whatever was the shape of gold colloids (spherical or nonspherical), silica shell growth always followed well the shape (or outline) of the gold colloids as shown in Fig. 1.

Absorption spectroscopy was used to check the position of the gold plasmon band after silica coating (Fig. 2). Au-20 nm@SiO_2-10 nm and Au-20 nm@SiO_2-25 nm nanoparticles exhibited a narrow plasmon band in the 520–530-nm region. A weak red shift was observed when silica thickness increased from 10 to 25 nm, due to the increase of the local refractive index around the gold colloids. The gold colloid plasmon band became broader with increasing diameter. This behavior can be attributed to the large shape distributions of 60- and 150-nm gold colloids, as previously discussed.

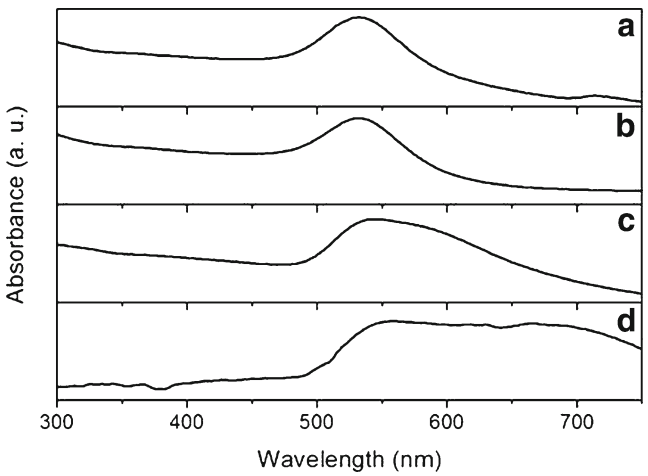

Fig. 2 Absorption spectra of $Au@SiO_2$ nanoparticles with various gold core diameters and silica shell thicknesses: **a** Au-20 nm@SiO_2-10 nm, **b** Au-20 nm@SiO_2-25 nm, **c** Au-60 nm@SiO_2-30 nm, and **d** Au-150 nm@SiO_2-15 nm

Synthesis of (Au@SiO_2)SiC Nanoparticles

As previously reported, silanol and carboxylic acid pending groups are present at the surface of SiC nanoparticles [21]. To achieve covalent immobilization of SiC nanoparticles onto $Au@SiO_2$ nanoparticles, carboxylic groups were first activated into NHS ester, and the $Au@SiO_2$ surface was modified with an aminosilane (APTMS) in order to bear amino groups. Ester-activated SiC nanoparticles and amino-modified $Au@SiO_2$ nanoparticles were reacted together in THF to form an amide bond (as already evidenced by IR spectroscopy [12]). Different amounts of SiC nanoparticles were added in order to test the influence of SiC density on (Au@SiO_2)SiC fluorescence properties. SiC reference dispersions were prepared at the same concentration to evaluate the enhancement factor. The absorption spectra of these SiC nanoparticle reference dispersions are shown in Fig. 3.

Absorbance was mainly located in the UV region as shown in Fig. 3. No well-defined peak was present, and

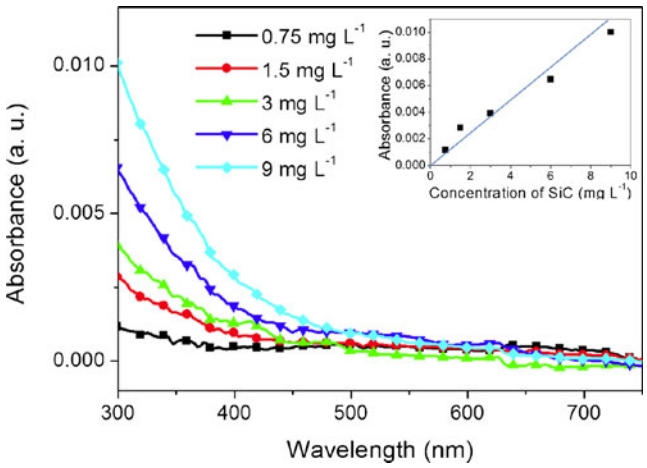

Fig. 3 Absorption spectra of SiC nanoparticle dispersions at different concentrations ranging from 0.75 to 9 mgL^{-1}. The *inset* shows the absorbance measured at λ=300 nm as a function of the concentration of SiC nanoparticles

only a long absorption tail was observed, which reflects the indirect nature of the SiC nanoparticle band gap [22]. Absorbance of SiC dispersion at λ=300 nm was found to be proportional to the concentration, in accordance with Beer–Lambert's law (insert in Fig. 3).

At a low concentration of SiC (0.75 to 9 mgL^{-1}), covalent immobilization of SiC nanoparticles onto Au@SiO_2 nanoparticles leads to the disappearance of the absorbance located in the UV region (Fig. 4). Only the gold plasmon band absorption peak above 500 nm was observed. At higher SiC concentrations (12 to 100 mgL^{-1}), the absorbance located in the UV region was still observed illustrating an excess of SiC nanoparticles in the dispersion, compared to the specific surface area of Au@SiO_2 nanoparticles available for SiC immobilization. The position of the gold plasmon band remained almost unchanged after covalent immobilization of SiC.

Fluorescence Properties

The fluorescence properties of SiC references and (Au@SiO_2)SiC nanoparticles were then compared. Excitation wavelength was set at 488 nm. Indeed, as previously demonstrated [12, 23], excitation must be chosen as close as possible to the gold plasmon band to observe an efficient enhancement. All fluorescence spectra exhibit intense Raman peaks around 585 nm, due to the water/ethanol dispersant [24], as shown in Fig. 5.

The broad band located between 550 and 750 nm corresponds to the fluorescence signal of SiC nanoparticles when excited at 488 nm. To extract the enhancement factor, the spectra were extrapolated in order to eliminate the Raman peaks' signal. This factor was determined by the ratio of (Au@SiO_2)SiC nanoparticles over the SiC nanoparticle intensities. When enhancement was high (as in Fig. 5a–d and g), a blue shift of the fluorescence spectrum was systematically obtained. The maximum was shifted from λ=582 nm for SiC nanoparticle references to λ=523 nm for (Au@SiO_2)

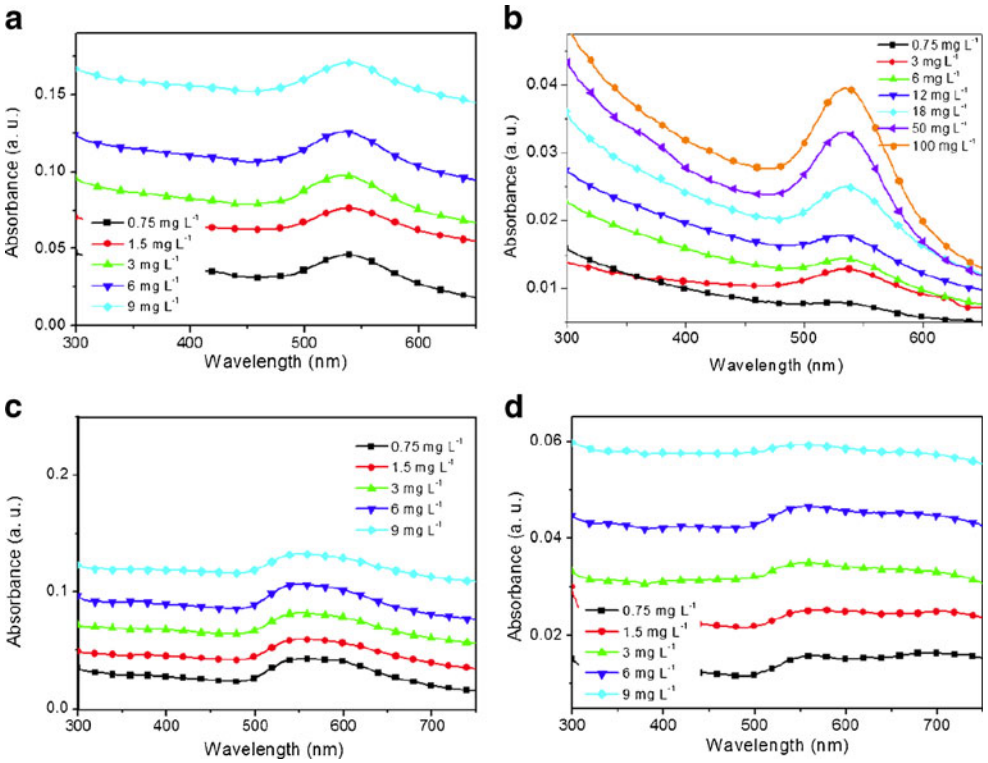

Fig. 4 Absorption spectra of (Au@SiO_2)SiC nanoparticles with various gold core diameters and silica shell thicknesses, and for different SiC nanoparticle concentrations: **a** Au-20 nm@SiO_2-10 nm, **b** Au-20 nm@SiO_2-25 nm, **c** Au-60 nm@SiO_2-30 nm, and **d** Au-150 nm@SiO_2-15 nm

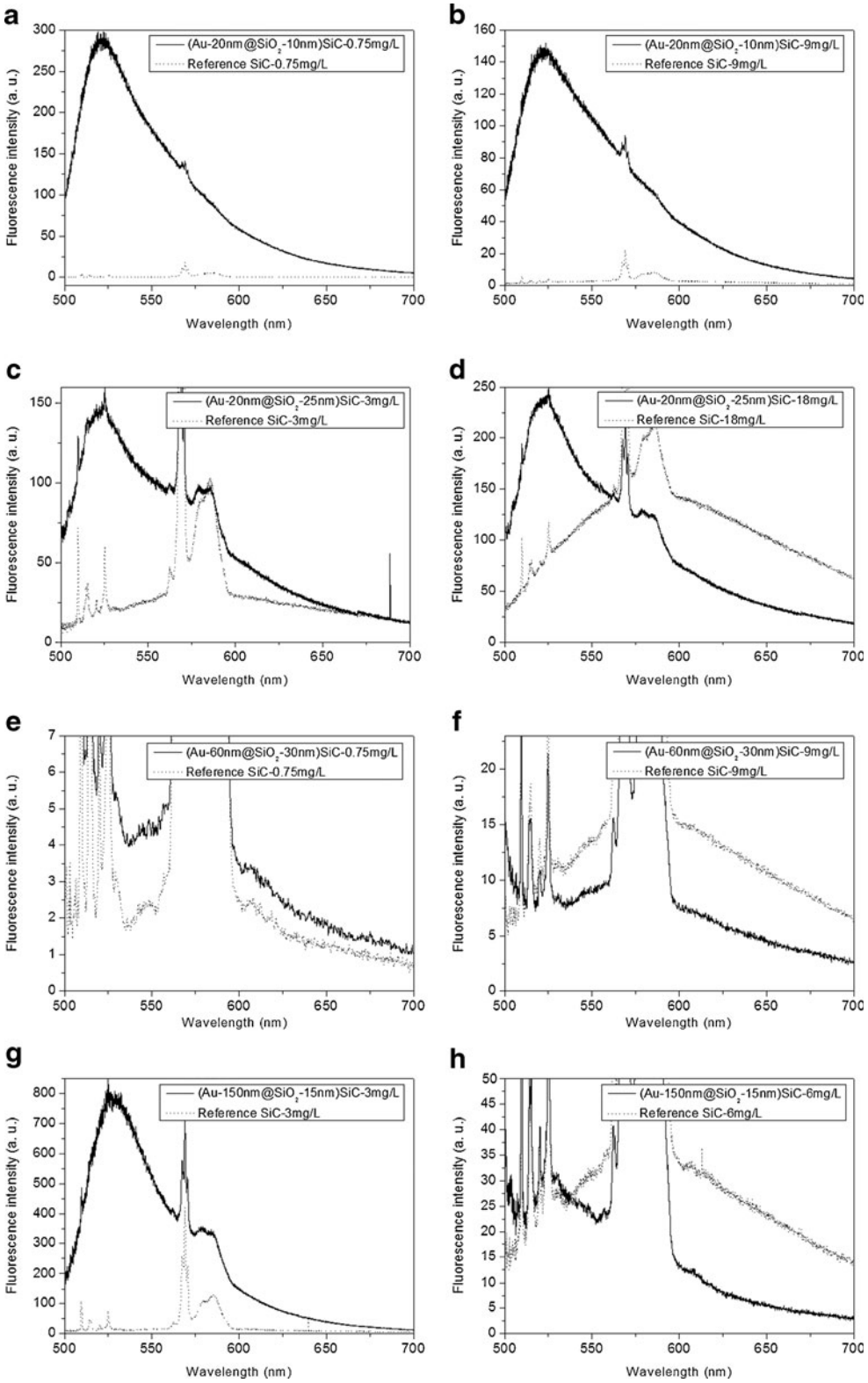

Fig. 5 Fluorescence spectra of ($Au@SiO_2$)SiC nanoparticles compared to references with the same concentrations of SiC nanoparticles: 20-nm gold core with 10-nm silica shell for **a** 0.75 and **b** 9 mgL^{-1}, 20-nm gold core with 25-nm silica shell for **c** 3 and **d** 18 mgL^{-1}, 60-nm gold core with 30-nm silica shell for **e** 0.75 and **f** 9 mgL^{-1}, 150-nm gold core with 15-nm silica shell for **g** 3 and **h** 6 mgL^{-1}

SiC nanoparticles. This blue shift was previously attributed to surface modification of SiC nanoparticles by their being covalently immobilized onto silica [12]. It was also shown that silica induced no significant enhancement. Thus, enhancement was calculated for these two emission wavelengths. For different core and shell diameters, enhancement factors as a function of SiC concentration are presented in Fig. 6.

Except for Au-150 nm@SiO_2-15 nm, the general trend was that enhancement factor decreased when SiC surface density was increased. Indeed, due to their large absorption

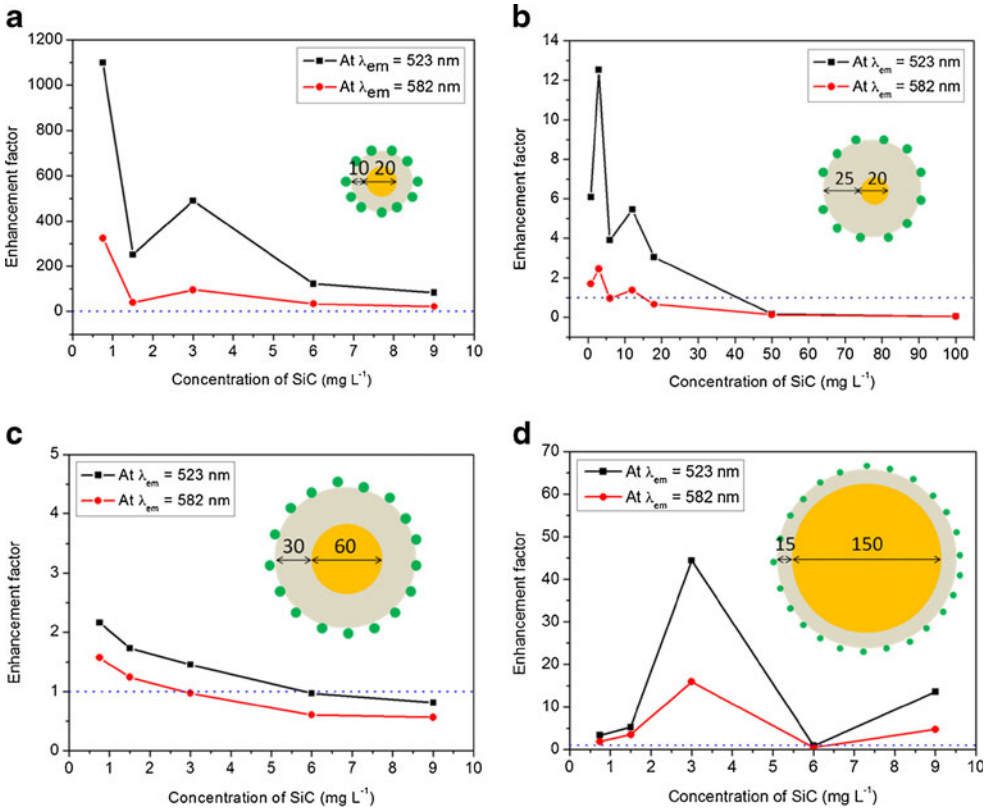

Fig. 6 Fluorescence enhancement factor as a function of SiC concentration (calculated at λ_{em}=523 nm and λ_{em}=582 nm) for various (Au@SiO_2)SiC nanoparticles: **a** Au-20 nm@SiO_2-10 nm, **b** Au-20 nm@SiO_2-25 nm, **c** Au-60 nm@SiO_2-30 nm, and **d** Au-150 nm@SiO_2-15 nm

and emission bands, SiC nanoparticles can be easily submitted to "self-quenching" because of the strong absorption–emission overlap in a broad wavelength range. This "self-quenching" can occur if the separation distance between two SiC nanoparticles is lower than 5 nm (Förster radius) [25]. Thus, when they are present in a large concentration, their fluorescence intensity decreased [26]. This can lead to quenching (enhancement factor lower than 1) in (Au@SiO_2)SiC nanoparticles when the SiC concentration is very high (50 and 100 mgL^{-1} as shown in Fig. 6b for Au-20 nm@SiO_2-25 nm).

Enhancement factor was strongly dependent on silica thickness and gold core diameter. For a 20-nm gold core, decreasing silica thickness from 25 to 10 nm induced a very strong increase of enhancement factor (about 300 at λ_{em}= 582 nm and more than 1,000 at λ_{em}=523 nm) as shown in Fig. 6a and b. For a 10-nm silica shell, the Au-SiC separation distance was optimized: strong plasmon-induced electric field and sufficient spacing to avoid quenching.

For Au-60 nm@SiO_2-30 nm nanoparticles, the enhancement factor becomes weaker (no more than 2 at λ_{em}=523 nm), which is probably due to the large spacing distance between gold and SiC (Fig. 6c). Moreover, due to the broad plasmon band, there is a strong overlap between SiC emission and gold plasmon, leading to possible quenching by Föster resonance energy transfer (FRET). For Au-150 nm@SiO_2-15 nm, surprisingly, an optimal SiC nanoparticle concentration was found at 3 mgL^{-1} (Fig. 6d). The explanation for this behavior could be that below 3 mgL^{-1}, the SiC concentration is too low compared to the diameter of Au@SiO_2 nanoparticles (total diameter, 180 nm). Therefore, at this concentration, we can suppose that the probability for SiC nanoparticles to meet the Au@SiO_2 surface is very weak. Thus, it is possible that most SiC nanoparticles were not covalently bonded to Au@SiO_2 and were eliminated during the washing step. When SiC concentration was larger than 3 mgL^{-1}, the weak enhancement obtained can be explained by self-quenching due to high SiC density.

Conclusion

In this paper, we have investigated the fluorescence-enhanced properties of (Au@SiO_2)SiC nanoparticles. The influence of several elaboration parameters was evaluated: gold core diameter, silica shell thickness, SiC nanoparticle concentration. The fluorescence spectra of (Au@SiO_2)SiC were blue-shifted compared to the fluorescence spectra of SiC nanoparticles. This was previously attributed to the surface modification of SiC nanoparticles when immobilized onto silica. Concerning the fluorescence enhancement, our results showed firstly that whatever is the gold core diameter, a 10–15-nm spacing between Au and SiC leads to maximum fluorescence enhancement, while a 25–30-nm spacing leads to weaker enhancement factors. Secondly, the broad plasmon band obtained for large-diameter gold nanoparticles (60 and

150 nm) induced weak enhancement factors. Indeed, in this case, the strong overlap between Au plasmon band and SiC emission band can lead to fluorescence quenching by FRET. Finally, the SiC concentration should be weak to avoid self-quenching. Thus, even if it appears that stronger plasmon-induced electric fields at the surface of bigger gold nanoparticles, the assumption that higher fluorescence enhancement can be obtained in this case is not always true. Other parameters, like the nature and the concentration of the fluorescent emitter, should also be taken into consideration.

References

1. Lakowicz JR, Geddes CD (2005) Radiative decay engineering. Vol. 8—topics in fluorescence spectroscopy. Springer, New York
2. Lakowicz JR (2006) Plasmonics in biology and plasmon-controlled fluorescence. Plasmonics 1:5–33
3. Lakowicz JR (2001) Radiative decay engineering: biophysical and biomedical applications. Anal Biochem 298:1–24
4. Bharadwaj P, Novotny L (2007) Spectral dependence of single molecule fluorescence enhancement. Opt Express 15:14266–14274
5. Tovmachenko OG et al (2006) Fluorescence enhancement by metal-core/silica-shell nanoparticles. Adv Mater 18:91–95
6. Liu N et al (2006) Hybrid gold/silica/nanocrystal-quantum-dot superstructures: synthesis and analysis of semiconductor–metal interactions. J Am Chem Soc 128:15362–15363
7. Zhang F et al (2010) Fabrication of $Ag@SiO_2@Y_2O_3$:Er nanostructures for bioimaging: tuning of the upconversion fluorescence with silver nanoparticles. J Am Chem Soc 132:2850–2851
8. Jin Y, Gao X (2009) Plasmonic fluorescent quantum dots. Nat Nanotechnol 4:571–576
9. Zhang J et al (2007) Metal-enhanced single-molecule fluorescence on silver particle monomer and dimer: coupling effect between metal particles. Nano Lett 7:2101–2107
10. Li C et al (2012) Metal-enhanced fluorescence of carbon dots adsorbed $Ag@SiO_2$ core-shell nanoparticles. RSC Adv 2:1765–1768
11. Nychyporuk T et al (2011) Strong photoluminescence enhancement of silicon quantum dots by their near-resonant coupling with multi-polar plasmonic hot spots. Nanoscale 3:2472–2475
12. Sui N et al. (2012) Plasmon-controlled fluorescence in ($Au@SiO_2$) SiC nanohybrids: enhanced, narrower and blue-shifted emission of SiC nanoparticles. J Nanopart Res 14:1004
13. Zhang Y et al (2011) Metal-enhanced photoluminescence from carbon nanodots. Chem Commun 47:5313–5315
14. Zakharko Y et al Plasmon-enhanced photoluminescence of SiC quantum dots for cell imaging applications. Plasmonics. doi:10.1007/s11468-012-9364-2
15. Frens G (1973) Controlled nucleation for the regulation of the particle size in monodisperse gold suspensions. Nature Phys Sci 241:20–22
16. Liz-Marzan LM et al (1996) Synthesis of nanosized gold-silica core-shell particles. Langmuir 12:4329–4335
17. Stöber W et al (1968) Controlled growth of monodisperse silica spheres in the micron size range. J Colloid Interface Sci 26:62–69
18. Botsoa J et al (2008) Application of 3C-SiC quantum dots for living cell imaging. Appl Phys Lett 92:173902
19. Westcott SL et al (1998) Formation and adsorption of clusters of gold nanoparticles onto functionalized silica nanoparticle surfaces. Langmuir 14:5396–5401
20. Patungwasa W, Hodak JH (2008) pH tunable morophology of the gold nanoparticles produced by citrate reduction. Mater Chem Phys 108:45–54
21. Zakharko Y et al (2010) Influence of the interfacial chemical environment on the luminescence of 3C-SiC nanoparticles. J Appl Phys 107:013503
22. Fan J et al (2008) 3C-SiC nanocrystals as fluorescent biological labels. Small 4:1058–1062
23. Maye MM et al (2010) Photoluminescence enhancement in CdSe/ZnS–DNA linked–Au nanoparticle heterodimers probed by single molecule spectroscopy. Chem Commun 46:6111–6113
24. Burikov S et al (2010) Raman and IR spectroscopy research on hydrogen bonding in water-ethanol systems. Mol Phys 108:2427–2436
25. Förster T (1965) Light and organic crystals: delocalized excitation and excitation transfer. Academic, New York
26. Botsoa J (2008) Synthèse de nanostructures de carbure de sillicium et étude de leurs propriétés optiques. PhD Dissertation, Institut National des Sciences Appliquées de Lyon